

Structure, motion, and multiscale search of traveling networks

Received: 18 November 2023

Accepted: 6 November 2024

Published online: 26 February 2025

Nate J. Cira¹✉, Morgan L. Paul^{2,10}, Shayandev Sinha^{3,11}, Fabio Zanini⁴,
Eric Yue Ma^{5,6,7} & Ingmar H. Riedel-Kruse^{8,9}✉

Network models are widely applied to describe connectivity and flow in diverse systems. In contrast, the fact that many connected systems move through space as the result of dynamic restructuring has received little attention. Therefore, we introduce the concept of ‘traveling networks’, and we analyze a tree-based model where the leaves are stochastically manipulated to grow, branch, and retract. We derive how these restructuring rates determine key attributes of network structure and motion, enabling a compact understanding of higher-level network behaviors such as multiscale search. These networks self-organize to the critical point between exponential growth and decay, allowing them to detect and respond to environmental signals with high sensitivity. Finally, we demonstrate how the traveling network concept applies to real-world systems, such as slime molds, the actin cytoskeleton, and human organizations, exemplifying how restructuring rules and rates in general can select for versatile search strategies in real or abstract spaces.

Network models play a key role in representing and understanding the characteristics of complex connected systems. Networks consist of ‘vertices’ connected by ‘edges’ (also termed ‘nodes’ and ‘links,’ respectively), and networks can be generated in different ways, for example, by randomly¹, regularly, or semi-randomly^{2–4} connecting existing vertices to each other. Processes of interest can often be understood using only the connectivity information between vertices⁵; however, additional constraints arise in spatial networks where each vertex is also embedded inside a real or abstract space⁶. Networks can be static or dynamically develop over time, for example, by iteratively branching from an initial seed^{7–14} as happens with neuronal dendrites¹⁴, branched organs¹⁵, or diffusion limited aggregation of particles⁸. Movement in the context of networks is usually discussed in terms of processes occurring on the network, for example, an agent walking over a network^{16,17} or information or disease spreading through a network^{18,19}. Despite significant work on temporal networks²⁰, surprisingly, there appears to be little systematic work on how networks

themselves travel through space away from an initial location *without* a permanently rooted anchor point.

Results

Traveling networks

We therefore introduce the concept of ‘traveling networks’—connected systems that change their location in space over time by rearranging their structure. This class of networks is motivated by various real-world systems, for example: (1) The slime mold *Physarum polycephalum* traverses the environment in search of food by rearranging its branched network (Fig. 1a, supplementary movie 1)^{21,22}. (2) The subcellular actin cytoskeleton network drives eukaryotic cell movement through polymerization and depolymerization of its filaments (Fig. 1b)^{23–25}. (3) Human corporations move through high-dimensional market spaces by creating new products and phasing out older ones (Fig. 1c)^{26–30}. For each of these systems, a characteristic time scale τ_r exists after which none of their original structure remains and the

¹Meinig School of Biomedical Engineering, Cornell University, Ithaca, NY, USA. ²Department of Bioengineering, Stanford University, Stanford, CA, USA. ³Rowland Institute, Harvard University, Cambridge, MA, USA. ⁴School of Clinical Medicine, UNSW Sydney, Sydney, NSW, Australia. ⁵Department of Physics, University of California, Berkeley, CA, USA. ⁶Department of EECS, University of California, Berkeley, CA, USA. ⁷Lawrence Berkeley National Laboratory, Berkeley, CA, USA. ⁸Department of Molecular and Cellular Biology, University of Arizona, Tucson, AZ, USA. ⁹Departments of Applied Mathematics, Biomedical Engineering, and Physics, University of Arizona, Tucson, AZ, USA. ¹⁰Present address: BridgeBio Pharma, Palo Alto, CA, USA. ¹¹Present address: Defect Metrology group, Intel Corporation, Hillsboro, OR, USA. ✉e-mail: njc222@cornell.edu; ingmar@arizona.edu

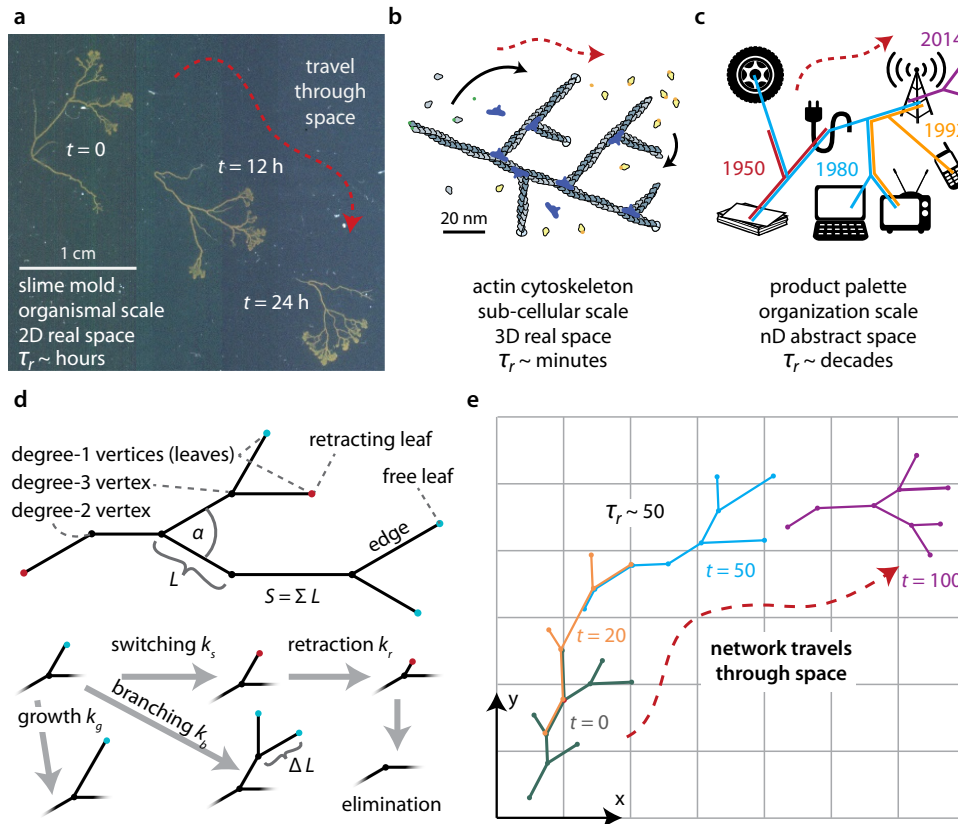


Fig. 1 | ‘Traveling networks’ that actively traverse space via dynamic restructuring are found in diverse contexts. a–c Examples of traveling networks: **a** a slime mold (2D real space)²¹, **b** actin cytoskeleton (3D real space)²³, **c** human organizations (high dimensional abstract space, depicting select products of Nokia Corporation over time)^{51–53}. **d** Model of a traveling network based on an acyclic binary tree with two leaf types. ‘Free leaves’ (cyan) branch at rate k_b , grow at rate k_g , and switch at

rate k_s , to become ‘retracting leaves’ (red) which retract at rate k_r until they reach a degree-three vertex. The branching angle is set by α , and the size of the network S is the sum of the edge lengths L . **e** The model from (d) results in a traveling network with conceptual similarity to (a–c). Time in arbitrary units. (a–c, e: Red arrow illustrates how networks travel through space; τ_r represents typical time scale after which the network has completely remodeled itself). (Image b inspired by^{23,54}).

network occupies a distinct new region of space (Fig. 1a–c). This makes these networks distinct from other well-studied networks that are able to dynamically grow and branch but do not leave their original rooted location^{7,9–14}.

A traveling network model

This motivates a deeper investigation into the constraints and opportunities experienced by such traveling networks. Here we propose and analyze a tractable model (Fig. 1d) that involves a tree with maximum degree (number of edges connected to a vertex) of three (supplementary sections 2, 3). The leaves (degree-one vertices) are stochastically manipulated and can be in either a ‘free’ or a ‘retracting’ state. Free leaves undergo three possible manipulations: (1) growth by adding unit length ΔL at rate k_g ; (2) branching at rate k_b , by creating two new free leaves—each with an edge of length ΔL at an angle $\pm \alpha/2$ from the previous edge, thereby converting the original leaf into a degree-three vertex; and (3) switching by becoming a retracting leaf at rate k_s . Retracting leaves undergo only one manipulation: removing length ΔL at rate k_r until they reach a degree-three vertex, upon which they are eliminated and generate a degree-two vertex. In this model, retracting leaves cannot switch back to being a free leaf. The amount of resources available to the system is represented by the overall size of the network, S , which is defined as the sum of all the edge lengths and implies that more spatially distant vertices require more resources to connect. S can be constant, or it can change over time depending on the system and external conditions. As the following analysis shows, the model’s restructuring rules lead to networks that exhibit characteristic dynamic structures (supplementary section 4), that travel

through space (supplementary sections 5, Fig. 1e, supplementary movie 2), and that effectively search this space (supplementary sections 6). This model clearly neglects many aspects of any particular real system (Fig. 1a–c), yet it proves to be very informative for analyzing many key properties and behaviors of general importance to traveling networks.

Network structure and criticality

We first systematically analyzed the network structure and dynamics (supplementary section 4). The network structure is characterized by the number of each of the different vertex types and their connectivity and can be crucial to network performance. We focused on the case where the network size S is constant, which implies that $k_b = k_s$. We considered a representation that is based on rates that are normalized by k_r (i.e., $K_B := k_b/k_r$, $K_G := k_g/k_r$, $K_S := k_s/k_r$, supplementary section 4.5.1). This allowed us to analyze the structure and behavior for networks of a given size in a phase space that is determined by just two independent restructuring parameters, i.e., $K_B := k_b/k_r$, $K_G := k_g/k_r$.

To visualize the network and confirm analytical results, we implemented a stochastic simulation embedded in 2D space (methods, supplementary section 8), though much of our analysis generalizes to higher spatial dimensions. We set $k_b = k_s$, and we numerically imposed preservation of size S by dynamically modifying the likelihood of switching up or down as needed (methods, supplementary section 8.1). We found that arbitrary starting configurations converge to steady state dynamics in which branching, growing, and retracting leaves cause the network to travel through space (supplementary movie 2). The observed network structures vary

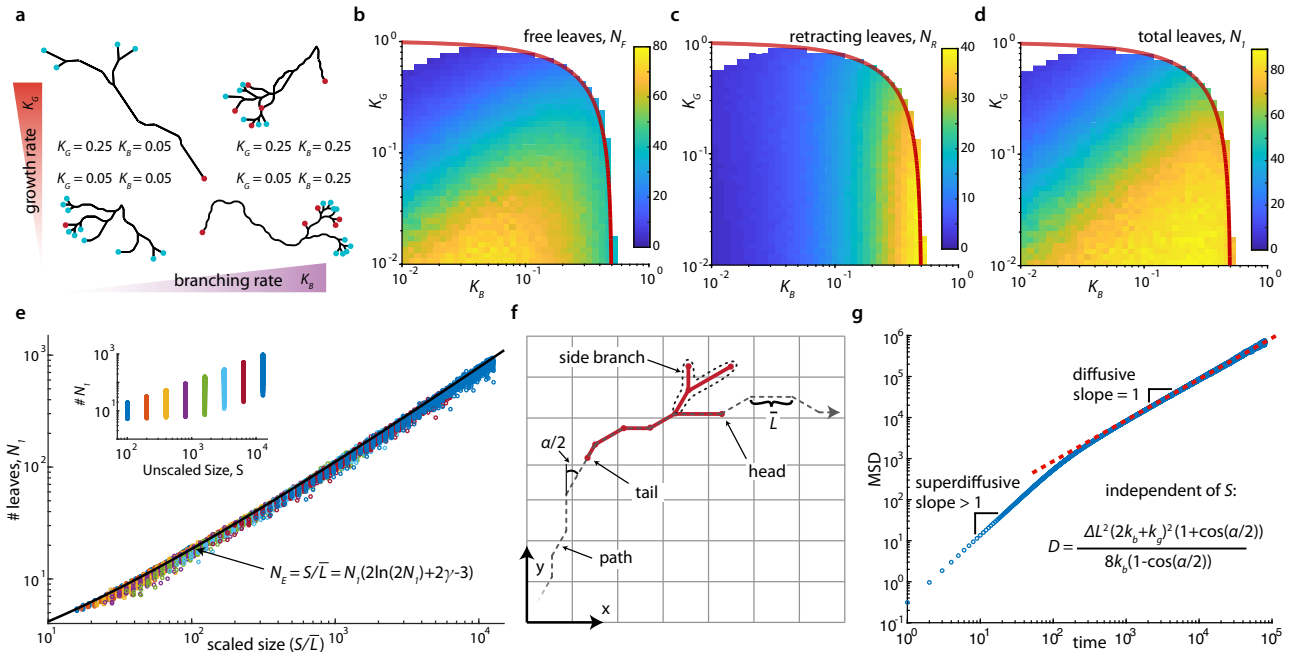


Fig. 2 | Network structure and movement are determined by restructuring rates. **a** A range of network structures are possible, illustrated by four typical networks at high/low K_B/K_G having different edge lengths, numbers of free leaves (cyan) and retracting leaves (red), and leaf type ratios (simulation of model from Fig. 1d; size, $S = 70$, supplementary movie 3). **b–d** K_B and K_G regulate the structure, exhibited by the mean numbers of free leaves (**b**), retracting leaves (**c**), and the total leaves (**d**) (simulated networks of $S = 800$; red lines: $2K_B + K_G \leq 1$ boundary of possible steady state behavior). **e** Total leaves, N_1 , for various sizes, S , across the steady-state

parameter space of K_B and K_G shown in (**b–d**). Number of leaves depends primarily on the average branch length \bar{L} as captured by the relation $S = N_1(2 \ln(2N_1) + 2\gamma - 3)$, where γ is the Euler-Mascheroni constant (black line). Inset: N_1 does not collapse with unscaled S . **f** The longer term network movement reveals a ‘tail’ and, in retrospect, a unique ‘path’, and a ‘head’ (supplementary movie 4). **g** The network (center of mass) moves superdiffusively over short time scales and diffusively over long time scales, with the diffusivity, D , set by $k_b, k_g, \Delta L$, and α . $k_b = 0.2, k_g = 0.1, \alpha = 60, S = 200$ shown here; red dashed line indicates analytical result.

characteristically with K_B and K_G as indicated by the number of retracting (N_R), free (N_F), and total ($N_1 = N_F + N_R$) leaves (Fig. 2a–d, supplementary movie 3); networks with high K_B have more retracting leaves; if both K_G and K_B are small, most leaves are free, and a large ratio of $K_G : K_B$ results in longer edges, fewer vertices, and fewer total leaves.

We then derived a set of analytical relationships between the model parameters that ultimately fully describe the network structure (supplementary sections 4.1–4.4), and we confirmed these relationships with simulations (methods, supplementary section 8). The edge lengths are distributed geometrically with mean length, $\bar{L} = \Delta L(1 + \frac{K_G}{2K_B}) = \Delta L \frac{2K_B + K_G}{2K_B}$. The number of all edges is $N_E = N_1 + N_2 + N_3 - 1$ (where N_i is the number of vertices of degree i), with $N_3 = N_1 - 2$ and $N_2 = N_E + 3 - 2N_1$, and on average $N_E = S/\bar{L}$. The ratio of the number of retracting to free leaves is $N_R/N_F = R = 2K_B + K_G = 2K_B\bar{L}$. By analyzing a recursive limit case, we found the final determining formula $S \approx N_1(2 \ln(2N_1) + 2\gamma - 3)$ (γ is the Euler-Mascheroni constant), which is in good agreement with simulations over the entire tested parameter space (Fig. 2e, supplementary section 4.4). The branching angle α (Fig. 1d) influences the embedding of the network in space but not the number of each vertex type or edge length distribution; embedding in higher dimensions leads to additional branching angles. Ultimately, the variables $\bar{L}, R, N_1, N_2, N_3, N_F, N_R$, and N_E are fully determined by just the three parameters K_G, K_B , and S , with \bar{L} and R even being independent of the network size S .

We note that the model can be fully non-dimensionalized using both the relevant time and length scales, not just k_r as above (supplementary section 4.5). This leads to just two independent parameters, i.e., the rescaled branching rate $K_B := \frac{k_b \bar{L}}{k_r \Delta L} = \frac{2k_b + k_g}{2k_r}$, and the total number of edges $N_E = S/\bar{L}$. Hence in case only networks of a given constant size S are considered, this even reduces to a single independent parameter. (The branching angle α could be considered an

additional parameter, but again only plays a role when embedding the network in space) All networks sharing these two parameters then belong to the same ‘universal form’ and show equivalent rescaled behavior (supplementary section 4.6). Since many real-world systems likely have more direct control over their specific rates than over N_E and K_B , we instead focus our remaining analysis on the earlier representation that is based on network size S and the original rates (k_b, k_g, k_r) or rates non-dimensionalized by k_r ($K_B := k_b/k_r, K_G := k_g/k_r$).

Importantly, we also found that these networks belong to a class of systems that automatically self-organize to operate at a critical point³¹. Size preservation and steady state require that the network remain balanced between exponentially increasing and exponentially decreasing the number of free leaves ($k_b = k_s$, supplementary section 4), reminiscent of a critical Galton-Watson process³². In the case of fast retraction, ($k_r \gg k_b$), the model exhibits features of self-organized criticality (SOC)³¹ with branching and retraction corresponding to slow driving and rapid relaxations (‘avalanches’), respectively (supplementary section 4.4.7). Utilizing the Riemann Zeta function, we found that the probability $P(L_R)$ of a retraction event of length L_R is scale-free, following the power law $P(L_R) = cL_R^a$, with $c \approx 0.74$ and $a \approx -2.48$ (supplementary section 4.4.7). Additionally, the network exhibits an approximately self-similar, fractal-like structure, which can be understood through the critical recursive dynamics by which the network travels and self-renews (supplementary section 4.4.8).

Network restructuring and traveling

Next, we analyzed how the network actually travels through space due to its branching, growing, retracting, and eventually disappearing leaves (supplementary section 5). One fundamental quantity for traveling networks is their relocation time, τ_r , the time it takes for the entire network to reorganize such that it occupies a new spatial position and none of its initial edges exist anymore (Fig. 1a–c, e).

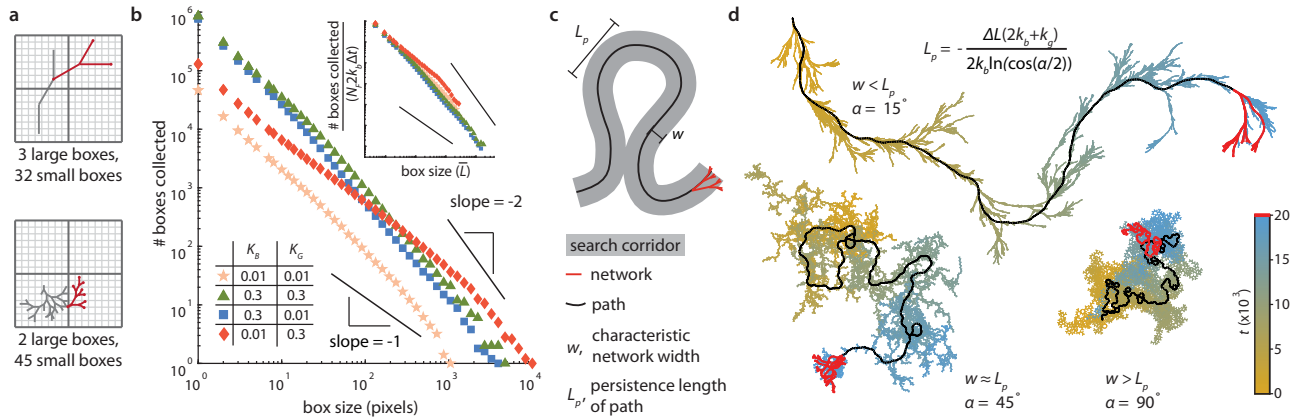


Fig. 3 | Traveling networks can control their passive search behavior across multiple length and time scales through regulation of their restructuring rates. **a** Schematic of box counting quantification over time illustrated for two different networks with different search efficacy at different spatial resolutions (gray is the full past history, and red is final network position). **b** Four networks, $S = 100$, runtime: $\Delta t = 2000$, $K_B = (0.01, 0.3)$, $K_C = (0.01, 0.3)$ show that having low k_b and high k_g maximizes diffusivity and collection of large boxes (red diamonds), and high k_b optimizes for collecting small boxes (blue squares and green triangles), illustrating a tradeoff between coarse and fine search. Low k_b and low k_g (peach stars) have worse performance across all sizes. (The slopes of -1 and -2 are

inserted for visual guidance). Inset: Rescaling box size by \bar{L} and boxes collected by $N_f \cdot 2k_b \cdot \Delta t$ (the total expected \bar{L} rescals) collapses this data onto a single curve. **c** Characteristic length scales of traveling networks include the network width, w , and path persistence length, L_p (supplementary sections 5.2.1 and 6.1.1). **d** Example networks of different w and L_p generated by varying branching angle, α (15, 45, 90 degrees) at constant $S = 200$, $k_b = 0.01$, $k_g = 0$, $k_r = 1$, $\Delta t = 20,000$. The most recently occupied historic network positions fade from blue (recent) to gold (old); red is the final position, and black indicates the path. For $w < L_p$, the network sweeps a search corridor along its path, and for $w > L_p$ the network behaves as a jittering blob.

Interestingly, we find that the relocation time depends only on the number of leaves and branching rate $\tau_r \approx \frac{N_l}{2k_b}$ (supplementary section 5.4). Another fundamental aspect is a description of the network's longer-term movement. In this acyclic model, for times larger than τ_r , we find that a single unique path exists that connects the network's initial and final positions (gray dashed line in Fig. 2f, supplementary movie 4). We define the 'tail' vertex as the oldest vertex in the network. The tail follows this unique path on the network's trailing end, advancing at rate k_r and intermittently pausing whenever it reaches a degree-three vertex. We also define a 'head' (which can only be identified in retrospect) as the free leaf that moved along this path at the leading edge of the network never switching or retracting. The head advances with speed $v_h = \Delta L(2k_b + k_g)$. To maintain a steady state length between head and tail along the path, $2k_b + k_g = f \cdot k_r$ must hold, where $f \leq 1$ is the fraction of time the tail is retracting rather than paused. In the framework nondimensionalized by k_r , this implies $2K_B + K_C \leq 1$, which constrains allowable values of K_B and K_C for steady state dynamics (red lines in Fig. 2b-d). Hence this type of network behaves like a chain of vertices moving along a random path while extending and retracting temporary side branches.

Focusing on the head dynamics, we identified a correlated random walk, which, over longer time scales, also corresponds to the motion of the network's center of mass. This random walk has step size \bar{L} , step rate $2k_b$, and turning angle $\alpha/2$. The diffusivity of the head and correspondingly the entire network can be written entirely in terms of the fundamental parameters as $D = \frac{\Delta L^2(2k_b + k_g)^2(1 + \cos(\alpha/2))}{8k_b(1 - \cos(\alpha/2))}$ (Fig. 2g), which corresponds to the freely rotating chain model in polymer physics^{33,34}. Interestingly, D is independent of network size. Networks with high k_g and low k_b diffuse fast (large D) but have structures with few free leaves (Fig. 2b). Having a small number of free leaves might be considered a risky configuration since it limits options for future directions of travel, and stochastic elimination of all free leaves at once could lead to catastrophic collapse of the entire network (methods, supplementary section 8). Together, the expressions derived above provide quantitative insights into the network's structure and motion, moreover, since the same rates simultaneously impact both structure and motion, this analysis highlights how traveling networks face inherent tradeoffs.

Passive spatial search

Such tradeoffs become particularly important for spatial search, a task that many traveling networks perform in real or abstract spaces (Fig. 1a-c, supplementary section 6.1). We therefore analyzed the efficacy of random search for different target sizes by counting all unique boxes of different sizes³⁵ that a network occupied within a given time period (Fig. 3a). We ran corresponding simulations on four networks with different combinations of high and low K_B and K_C (Fig. 3b). The low K_B , high K_C network collected the most large boxes, which can be understood through the expression for D , which indicates larger diffusivity for large K_C . Networks with higher K_B collected the most small boxes since new lengths of \bar{L} are added at rate $N_f \cdot 2k_b$ (before the network begins crossing itself). The low K_B , low K_C network diffuses slowly and does not add much length per time hence it is not an effective searcher at any length scale. Data from all four networks actually collapse to a single curve when rescaled, corresponding to the universal form discussed earlier (Fig. 3b inset, supplementary sections 4.6 and 6.1). The absolute value of the slope of these plots is the Hausdorff dimension of the network history which increases toward 2 with long runtimes as self-crossing becomes more frequent (supplementary section 6.1.4), consistent with Brownian trails in two or more dimensions³⁵. Hence traveling networks can tune their restructuring rates for optimal multiscale search depending on the relevant time and length scales.

Network size and branching angle affect how much space the side branches can explore, thus we analyzed how these parameters impact search behavior. Using the above expressions and understanding of the network's structure and motion, we find that the path has a characteristic persistence length, $L_p = -\bar{L} / \ln(\cos(\alpha/2))$, and the network has a characteristic search width, w , (Fig. 3c) which itself has a more complex dependence on \bar{L} , α , and S (supplementary section 6.1.1). For $w < L_p$ the network behaves like a particle sweeping a corridor, and for $w > L_p$ the network behaves like a jittering blob conducting a fine-scale search of limited scope, reminiscent of tradeoffs in depth-first and breadth-first search strategies³⁶. This 'search morphology' is sensitive to α as illustrated in Fig. 3d. Counting boxes of size $\bar{L} = 1$ over time reveals that the optimal angle for search depends on the search duration, with $w \approx L_p$ collecting more boxes over shorter times and $w < L_p$ collecting more boxes over longer times in these examples (supplementary section 6.1.5).

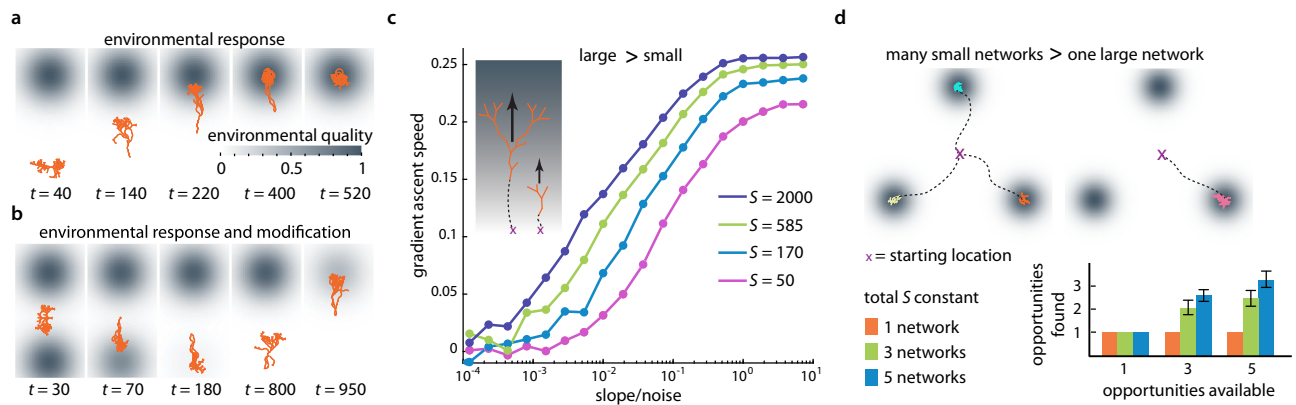


Fig. 4 | Traveling networks can control their active search behavior across multiple length and time scales through regulation of their restructuring rates. **a, b** Traveling networks can perform biased search by making leaf switching rates depend on the local vs. globally sensed environment in a stationary gradient (a) or even while modifying their environment (b). **c** When ascending a noisy

gradients, large networks tolerate lower slope-to-noise-ratios and ascend faster than small networks. Different network sizes: S , $\alpha = 60^\circ$, $k_b = 0.1$, $k_g = 0$. **d** Multiple small networks exploit more opportunities in environments with multiple opportunities than a single large network of the same total size. ($n = 40$ trials, error bars are one standard deviation).

Active and biased spatial search

Beyond the random restructuring and motion considered so far, we now consider traveling networks that respond to their environments through biased restructuring (supplementary section 6.2). We extended the model by making the free leaves sense and respond to variations in the environment. Here the switching rate of every free leaf increases or decreases depending on whether the environment, represented by a scalar field, at that leaf's position is smaller or larger, respectively, compared to the field averaged across all free leaves. This leads to a biased motion of the network up a field gradient (Fig. 4a, supplementary movie 5, methods, supplementary section 8.4.1). To capture environmental resource consumption as caused by natural systems (Fig. 1a)^{21,22}, we coupled the network position to modifications of the field itself, leading to the network's biased motion through a changing environment (Fig. 4b, supplementary movie 6).

Many other model alterations can capture various environmental responses. For example, in an alternative model we modified the rates based on only local information and allowed the network's size S (which was kept constant until now) to change in response to a dynamic environment (supplementary movie 7, methods, supplementary section 8.4.2). This is akin to a *Physarum* network (Fig. 1a) that moves in response to food in the environment, changes its network size accordingly, and modifies the food distribution in the environment by consumption²¹. A deeper and more systematic analysis of such networks is left for future work (supplementary section 7.2).

Importantly, these traveling networks can function as highly sensitive detectors as network size preservation self-organizes³⁷ (or 'self-tunes'³⁸) them to operate at a critical point where small environmentally-induced changes to their fundamental underlying restructuring rates can cause enormous changes to their emergent structure and motion through local exponential growth and decay (supplementary section 6.2). Note that even when network size is not preserved, such critical behavior and thereby sensitivity could be implemented locally within subsets of the network.

Many real-world traveling networks (Fig. 1a–c) can split into multiple smaller entities or merge into larger structures (Fig. 1a, c)^{21,39}, suggesting that trade-offs exist between network size and network number for performing efficient search tasks. We tested this hypothesis with simulations (Fig. 4c, d). We found that for responsive networks moving up a linear, noisy gradient, larger networks are able to move faster and tolerate higher noise levels than smaller networks (Fig. 4c). However, in a landscape with different numbers of 'opportunities', represented by local Gaussian maxima, multiple small

networks are able to capture more opportunities than a single large network of the same total size (Fig. 4d, supplementary movie 8). Hence it can be more advantageous to allocate the resources into one large network or into multiple smaller networks - depending on the specific environment and search task.

Application to real-world systems

Connecting the traveling network concept and our analysis results back to our motivating examples (Fig. 1a–c), we note that evidence for similar connections between underlying parameters choices, network structure, and strategic movements exists in the literature (Fig. 5a–c). (1) Takamatsu et al.¹⁰ experimentally observed that *Physarum* adopts different network structures depending on its environment. More highly branched sheet-like networks formed under favorable nutrient-rich conditions contrasting with longer, spindly networks that formed in adverse chemical environments (Fig. 5a) (supplementary movies 7 and 9). (2) The actin literature connects (de-) polymerization and branching rates to cytoskeletal structure and movement, which then affect the number of filopodia and higher-level (search) behaviors of cells (Fig. 5b)^{24,40}. There is also experimental evidence for SOC in actin networks⁴¹ similar to our model predictions (supplementary section 4.4). (3) The business strategy literature identified a positive correlation between shareholder returns and capital reallocation among a company's business units (Fig. 5c)^{42,43}, suggesting that active movement through the space of market opportunities via dynamic changes (termed 'seeding', 'nurturing' and 'pruning') is important for productivity. Additionally, there is also analysis of which factors make it advantageous for companies to merge or split (compare to Fig. 4c, d)^{44,45}. In the context of a traveling network model, we identify how rates (k_b , k_g , k_r) should be changed in order to select the desired behavioral strategy (Fig. 5a–c). Conclusions from the model analyzed here can be summarized in a concise 2D parameter space (Fig. 5d) (supplementary sections 4.5.2 and 4.6) that reveals various trade-offs, such as between coarse fast search vs. fine slow search or when switching between 'exploration and exploitation'⁴⁶ or when avoiding the risk of catastrophic collapse by operating sufficiently far away from non-steady state conditions at the expense of slower dynamics overall (red line, Fig. 5d).

Alternative models

So far, our analysis focused on one model with particular assumptions (Fig. 1d), but many real-world traveling networks likely follow very different restructuring rules. As a contrasting example, we analyzed a similar model in which retracting leaves were also allowed to revert back into being growing and branching leaves. Hence in this altered

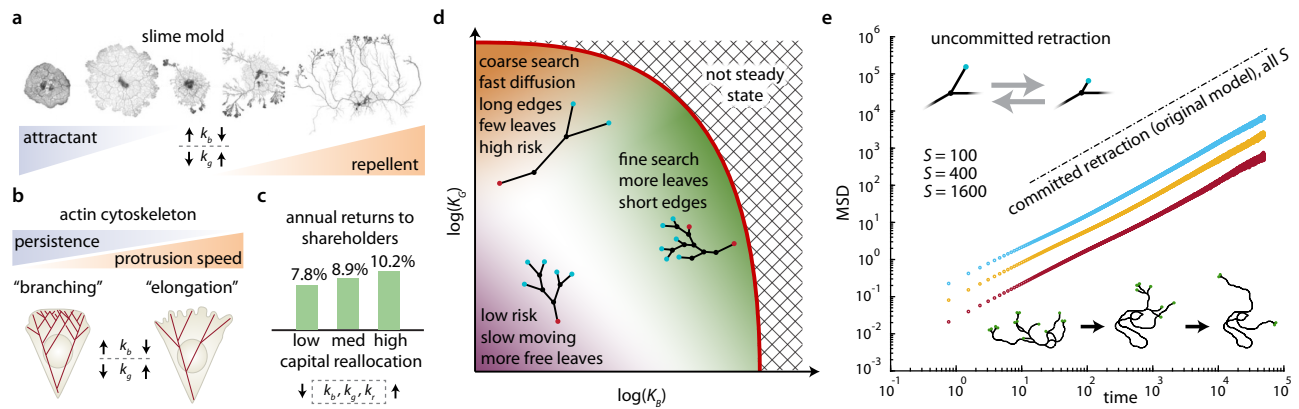


Fig. 5 | Real-world traveling networks can optimize for different behaviors through dynamic changes to their restructuring rates. **a** Different *Physarum* network morphologies are seen in adverse and favorable environments (right vs. left)¹⁰. **b** Changes in actin cytoskeleton structure and resulting cell movement due to network restructuring by branching and elongation⁴⁰. **c** Positive association between more capital reallocation (higher restructuring rates) and returns for corporations, 1990–2005, based on three quantiles of $n = 1616$ companies⁴². (Images in (a–c) adapted from the corresponding references. Up and down arrows indicate how restructuring rates might be changed within a traveling network

model to achieve the behaviors; rate changes deduced qualitatively from the literature^{10,40,42,43}. **d** Summary of behavioral and ecologically relevant network properties and their codependence on the underlying restructuring rates in a concise 2D parameter space (example network morphologies superimposed, overall conclusions independent of S ; colors of vertices as in Fig. 1d, time nondimensionalized by k_r). **e** A traveling network model without persistent retraction ('uncommitted retraction' model) explores the space more slowly than the original model (Fig. 1d), and becomes even less efficient with increasing network size.

model only one leaf type exists, and leaves frequently alternate back and forth between retraction and growth (Fig. 5e). We found that for such an 'uncommitted retraction' model the resulting networks do not display the range of morphologies seen in Fig. 2a; instead these networks degenerate into a single chain of nearly unbranched degree-two vertices (Fig. 5e inset, supplementary section 7.1, supplementary movie 10). Furthermore, the diffusion rate significantly slows with increasing network size S , unlike the much faster and size-independent diffusion of the original model (Figs. 2g and 5e). Hence the 'stay committed to retraction once started' rule appears important here for achieving structural complexity as well as for effective motion and search, and, more broadly, rules as well as rates can have a profound impact on traveling network performance.

Discussion

In summary, here we introduced the concept of traveling networks. We then proposed an accessible mathematical model for such systems, and our analysis uncovered and quantitatively explains numerous features: The network traverses through space with a diffusive motion that is independent of network size and with a characteristic restructuring time after which complete network self-renewal occurs. Thereby, an approximately self-similar, fractal-like network structure emerges, which allows for effective and distributed search across multiple length scales. Such search can be highly sensitive and responsive to environmental signals as the network self-organizes to a critical point. We then showed analytically how many of these key structural and dynamic properties emerge from the underlying restructuring rules and restructuring rates. This set of highly complex network dynamics and strategies can ultimately be reduced to a simple two-dimensional behavioral space, which provides a direct connection between restructuring rates and network performance (Fig. 5d; supplementary section 4.6).

Multiple of these results depend on the specific model (Fig. 5e). Hence alternative rule choices and more complex environmental scenarios should be investigated in the future (supplementary section 7.2), which promises a rich set of theoretical results and applied insights into this class of systems. In particular, we believe that this traveling network concept can aid the deeper understanding and the optimization of various natural and artificial dynamic systems beyond the examples discussed so far (Figs. 1a–c and 5a–c), such as

interbreeding populations traveling through the space of genotypes⁴⁷, swarm robots restructuring their communication tree⁴⁸, or researchers and labs pursuing different strategies when traveling through 'knowledge space' with presumed correlations for scientific impact^{46,49}.

Methods

Numerical implementation of the model

We simulated the dynamics of the traveling network model introduced in the text with a stochastic algorithm implemented in MATLAB. Details of this implementation can be found in the supplementary material, and the code can be found on GitHub as described in "Code Availability".

Cultivation and analysis of *Physarum*

P. polycephalum was cultivated as in Hossian et al.²¹. Briefly, *P. polycephalum* (Carolina Biological Supply) was maintained on oat flakes and inoculated onto 2% non-nutrient agar (BD Bacto Agar). An HP Scanjet G3110 flatbed scanner was used to record the behavior, taking images every 10 min. In supplementary movie 9, food was deposited as droplets of oatmeal water with a custom robotic setup and indicated by a digital overlay, as described in Hossian et al.²¹.

Image analysis for displaying the 'age' of different parts of the organism in supplementary movie 1 was performed by subtracting the background from images, then extracting the pixels representing the organism from these images using the 'ilastik' pixel classifier⁵⁰ trained on 19 labeled *physarum* images. Pixel age as in supplementary movie 1 was defined as the number of frames that a particular pixel had been occupied. The organism path was extracted manually.

Reporting summary

Further information on research design is available in the Nature Portfolio Reporting Summary linked to this article.

Data availability

The authors declare that the data supporting the findings of this study are available within the paper and its Supplementary Information files. Should any raw data files be needed in another format they are available from the corresponding author upon request.

Code availability

A MATLAB script that simulates the base traveling network model is available at: <https://github.com/CiraLab/TravelingNetworks>.

References

- Erdős, P. & Rényi, A. On random graphs i. *Publ. Math.* **6**, 290–297 (1959).
- Watts, D. J. & Strogatz, S. H. Collective dynamics of ‘small-world’ networks. *Nature* **393**, 440–442 (1998).
- Price, D. S. A general theory of bibliometric and other cumulative advantage processes. *J. Assoc. Inf. Sci. Technol.* **27**, 292–306 (1976).
- Barabási, A.-L. & Albert, R. Emergence of scaling in random networks. *Science* **286**, 509–512 (1999).
- Milo, R. et al. Network motifs: simple building blocks of complex networks. *Science* **298**, 824–827 (2002).
- Barthélemy, M. Spatial networks. *Phys. Rep.* **499**, 1–101 (2011).
- Eden, M. A two-dimensional growth process. *Proc. Fourth Berkeley Symp. Math. Statist. Prob.* **4**, 223–239 (1961).
- Witten Jr, T. A. & Sander, L. M. Diffusion-limited aggregation, a kinetic critical phenomenon. *Phys. Rev. Lett.* **47**, 1400 (1981).
- Cuntz, H., Forstner, F., Borst, A. & Häusser, M. One rule to grow them all: a general theory of neuronal branching and its practical application. *PLoS Comput. Biol.* **6**, e1000877 (2010).
- Takamatsu, A., Takaba, E. & Takizawa, G. Environment-dependent morphology in plasmodium of true slime mold *Physarum polycephalum* and a network growth model. *J. Theor. Biol.* **256**, 29–44 (2009).
- Mandelbrot, B. B. *The Fractal Geometry of Nature* (WH freeman New York, 1982).
- Meinhardt, H. *Models of Biological Pattern Formation* (Academic Press, 1982).
- Cardy, J. L. & Täuber, U. C. Field theory of branching and annihilating random walks. *J. Stat. Phys.* **90**, 1–56 (1998).
- Shree, S. et al. Dynamic instability of dendrite tips generates the highly branched morphologies of sensory neurons. *Sci. Adv.* **8**, eabn0080 (2022).
- Hannezo, E. et al. A unifying theory of branching morphogenesis. *Cell* **171**, 242–255 (2017).
- Lovász, L. Random walks on graphs. *Comb., Paul Erdős Eighty* **2**, 4 (1993).
- Starnini, M., Baronchelli, A., Barrat, A. & Pastor-Satorras, R. Random walks on temporal networks. *Phys. Rev. E* **85**, 056115 (2012).
- Pastor-Satorras, R. & Vespignani, A. Epidemic spreading in scale-free networks. *Phys. Rev. Lett.* **86**, 3200 (2001).
- Newman, M. E. Spread of epidemic disease on networks. *Phys. Rev. E* **66**, 016128 (2002).
- Holme, P. & Saramäki, J. Temporal networks. *Phys. Rep.* **519**, 97–125 (2012).
- Hossain, Z. et al. Interactive cloud experimentation for biology: an online education case study. In *Proceedings of the 33rd Annual ACM Conference on Human Factors in Computing Systems*, 3681–3690 <https://doi.org/10.1145/2702123.2702354> (2015).
- Alim, K., Amselem, G., Peaudecerf, F., Brenner, M. P. & Pringle, A. Random network peristalsis in *Physarum polycephalum* organizes fluid flows across an individual. *Proc. Natl. Acad. Sci.* **110**, 13306–13311 (2013).
- Pollard, T. D. & Cooper, J. A. Actin, a central player in cell shape and movement. *Science* **326**, 1208–1212 (2009).
- Carlier, M.-F. & Shekhar, S. Global treadmilling coordinates actin turnover and controls the size of actin networks. *Nat. Rev. Mol. Cell Biol.* **18**, 389–401 (2017).
- Mohapatra, L., Goode, B. L., Jelenkovic, P., Phillips, R. & Kondev, J. Design principles of length control of cytoskeletal structures. *Annu. Rev. Biophys.* **45**, 85–116 (2016).
- Hannan, M. T. & Freeman, J. The population ecology of organizations. *Am. J. Sociol.* **82**, 929–964 (1977).
- Carroll, G. R. Concentration and specialization: dynamics of niche width in populations of organizations. *Am. J. Sociol.* **90**, 1262–1283 (1985).
- Peli, G. & Nooteboom, B. Market partitioning and the geometry of the resource space. *Am. J. Sociol.* **104**, 1132–53 (1999).
- Penrose, E. T. *The Theory of the Growth of the Firm* (Oxford University Press, 2009).
- Helfat, C. E. & Eisenhardt, K. M. Inter-temporal economies of scope, organizational modularity, and the dynamics of diversification. *Strateg. Manag. J.* **25**, 1217–1232 (2004).
- Bak, P., Tang, C. & Wiesenfeld, K. Self-organized criticality: an explanation of the 1/f noise. *Phys. Rev. Lett.* **59**, 381 (1987).
- Athreya, K. B. & Ney, P. E. *Branching Processes* (Springer Berlin Heidelberg, 1972).
- Doi, M. & Edwards, S. F. *The Theory of Polymer Dynamics*, Vol. 73 (Oxford University Press, 1988).
- Gedde, U. W. *Polymer Physics* (Springer, Dordrecht, 1999).
- Falconer, K. *Fractal Geometry: Mathematical Foundations and Applications* (John Wiley & Sons, 2004).
- Jungnickel, D. & Jungnickel, D. *Graphs, Networks and Algorithms*, Vol. 3 (2005).
- Mora, T. & Bialek, W. Are biological systems poised at criticality? *J. Statist. Phys.* **144**, 268–302 (2011).
- Camalet, S., Duke, T., Jülicher, F. & Prost, J. Auditory sensitivity provided by self-tuned critical oscillations of hair cells. *Proc. Natl. Acad. Sci.* **97**, 3183–3188 (2000).
- Daepf, M. I., Hamilton, M. J., West, G. B. & Bettencourt, L. M. The mortality of companies. *J. Royal Soc. Interface* **12**, 20150120 (2015).
- Krause, M. & Gautreau, A. Steering cell migration: lamellipodium dynamics and the regulation of directional persistence. *Nat. Rev. Mol. Cell Biol.* **15**, 577–590 (2014).
- Cardamone, L., Laio, A., Torre, V., Shahapure, R. & DeSimone, A. Cytoskeletal actin networks in motile cells are critically self-organized systems synchronized by mechanical interactions. *Proc. Natl. Acad. Sci.* **108**, 13978–13983 (2011).
- Hall, S., Lovallo, D. & Musters, R. How to put your money where your strategy is. *McKinsey Quarterly* **2**, 28–38 (2012).
- Bradley, C., Hirt, M. & Smit, S. Strategy to beat the odds. *McKinsey Quarterly* **12**, 28–38 (2018).
- Harford, J. What drives merger waves? *J. Financ. Econ.* **77**, 529–560 (2005).
- Mitchell, M. L. & Mulherin, J. H. The impact of industry shocks on takeover and restructuring activity. *J. Financ. Econ.* **41**, 193–229 (1996).
- Liu, L., Dehmamy, N., Chown, J., Giles, C. L. & Wang, D. Understanding the onset of hot streaks across artistic, cultural, and scientific careers. *Nat. Commun.* **12**, 1–10 (2021).
- Schluter, D. Evidence for ecological speciation and its alternative. *Science* **323**, 737–741 (2009).
- Rubenstein, M., Cornejo, A. & Nagpal, R. Programmable self-assembly in a thousand-robot swarm. *Science* **345**, 795–799 (2014).
- Zeng, A. et al. Increasing trend of scientists to switch between topics. *Nat. Commun.* **10**, 1–11 (2019).
- Sommer, C., Straehle, C., Koethe, U. & Hamprecht, F. A. Ilastik: interactive learning and segmentation toolkit. In *2011 IEEE international symposium on biomedical imaging: From nano to macro*, 230–233 (IEEE, 2011). <https://ieeexplore.ieee.org/abstract/document/5872394>.
- Häikiö, M. *Nokia-the Inside Story* (Edita, 2002).
- Steinbock, D. *The Nokia Revolution: The Story of an Extraordinary Company that Transformed an Industry* (AMACOM, New York, 2001).
- Doz, Y. & Wilson, K. *Ringtone: Exploring the Rise and Fall of Nokia in Mobile Phones* (Oxford University Press, 2017).
- Mbinfo. (Accessed 04 June 2023); <http://mechanobio.info/>.

Acknowledgements

The authors gratefully acknowledge helpful comments from W. Gilpin, J. Deacon, A. Yankovic, J.T. Morton, S.H. Strogatz, and J. Dunkel. Z. Hossain and X. Jin provided assistance with Physarum experiments. M.L.P. and N.J.C. were supported by NSF GRFP Fellowships (DGE-1656518). N.J.C. was supported by a Siebel Scholars Fellowship and a Rowland Fellowship. I.H.R.K. acknowledges support from NSF grants 2214020, and 2229070, and NIH grant 1R01GM145893.

Author contributions

N.J.C., E.Y.M., and I.H.R.K. jointly conceived the project. N.J.C. and I.H.R.K. performed mathematical derivations with input from F.Z., M.L.P., and S.S. N.J.C. implemented and ran simulations with input from M.L.P. and S.S. N.J.C. and S.S. collected data from simulations. N.J.C. and I.H.R.K. wrote the paper with input from E.Y.M., F.Z., M.L.P., and S.S. All authors made intellectual contributions.

Competing interests

The authors declare no competing interests.

Additional information

Supplementary information The online version contains supplementary material available at <https://doi.org/10.1038/s41467-024-54342-7>.

Correspondence and requests for materials should be addressed to Nate J. Ciria or Ingmar H. Riedel-Kruse.

Peer review information *Nature Communications* thanks Xiangyi Meng and Thilo Gross for their contribution to the peer review of this work. A peer review file is available.

Reprints and permissions information is available at <http://www.nature.com/reprints>

Publisher's note Springer Nature remains neutral with regard to jurisdictional claims in published maps and institutional affiliations.

Open Access This article is licensed under a Creative Commons Attribution-NonCommercial-NoDerivatives 4.0 International License, which permits any non-commercial use, sharing, distribution and reproduction in any medium or format, as long as you give appropriate credit to the original author(s) and the source, provide a link to the Creative Commons licence, and indicate if you modified the licensed material. You do not have permission under this licence to share adapted material derived from this article or parts of it. The images or other third party material in this article are included in the article's Creative Commons licence, unless indicated otherwise in a credit line to the material. If material is not included in the article's Creative Commons licence and your intended use is not permitted by statutory regulation or exceeds the permitted use, you will need to obtain permission directly from the copyright holder. To view a copy of this licence, visit <http://creativecommons.org/licenses/by-nc-nd/4.0/>.

© The Author(s) 2025